

# Relative stability of $\alpha$ and $\beta$ boron

Michael Widom<sup>1</sup>

Marek Mihalkovič<sup>2</sup>

<sup>1</sup> Department of Physics, Carnegie Mellon University, Pittsburgh PA 15213, USA

<sup>2</sup> Department of Physics, Slovakian Academy of Sciences, Bratislava Slovakia

E-mail: [widom@andrew.cmu.edu](mailto:widom@andrew.cmu.edu)

**Abstract.**  $\alpha$  and  $\beta$  rhombohedral boron are closely related structures with nearly identical stability. Unlike  $\alpha$ , in which every site is fully occupied,  $\beta$  is characterized by partial occupancy and intrinsic disorder. Optimizing the site occupation yields a superstructure of  $\beta$  that we call  $\beta'$ . Its energy is lower than  $\alpha$  but its symmetry lower than  $\beta$ . The configurational entropy of partial occupation drives a  $\beta' \rightarrow \beta$  transition around room temperature. Comparing the vibrational density of states, we find that  $\beta'$  has an excess of low frequency modes that are strongly localized around the partially occupied sites. The vibrational entropy of these low frequency modes adds to the configurational entropy of partial occupation to further stabilize the  $\beta'$  structure compared to  $\alpha$ .

## 1. Introduction

The relative stability of  $\alpha$  and  $\beta$  rhombohedral boron has long puzzled researchers [1, 2, 3]. While  $\beta$  is observed experimentally to be the stable phase and remain so down to low temperatures, initial calculations of total energies [4, 5, 6] found  $E_\alpha < E_\beta$ . The  $\beta$  structure was taken as Pearson type hR105, which is rhombohedral with 105 atoms in the 105-site primitive cell [7]. However, improved crystallographic studies of the  $\beta$  phase reveal partially occupied sites [8, 9], leading to Pearson type hR141 with approximately 107 atoms distributed among 141 sites. By optimizing the placement of atoms on these sites a variant of  $\beta$  (henceforth named  $\beta'$ ) is found with  $E_{\beta'} < E_\alpha$ , indicating that the true ground state is likely a superstructure of  $\beta$  with a specific symmetry-broken assignment of atoms among the partially occupied sites [10]. We propose that the symmetric  $\beta$  phase is restored above a moderate temperature and stabilized relative to  $\beta'$  by the entropy of partial site occupation.

The hR12 structure of  $\alpha$ -boron shown in Fig. 1 is relatively simple with just 2 Wyckoff positions (i.e. 2 separate groups of symmetry-equivalent atomic sites) and a total of 12 atomic sites per rhombohedral cell. Every atomic site is fully occupied. In contrast, the hR141 structure [9] of  $\beta$  comprises 20 Wyckoff positions labeled B1-B20. Wyckoff positions B1-B15 coincide with those of the earlier hR105 structure [7]. Site B15 occupies the rhombohedral cell center. The sites reported to be partially occupied are B13 and B16-20, and are color-coded according to occupancy in Fig. 2.

The following section of this paper reviews the proposed optimized  $\beta'$  structure and its discrete low-lying excitations related to changes in site occupation. However, the complete configuration space is continuous, owing to the phonon degrees of freedom and their associated vibrational free

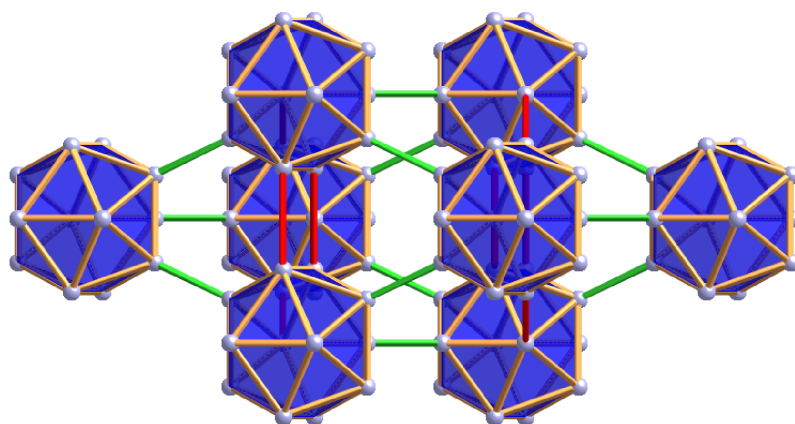


**Figure 1.** Structure of  $\alpha$ -B (Pearson hR12).

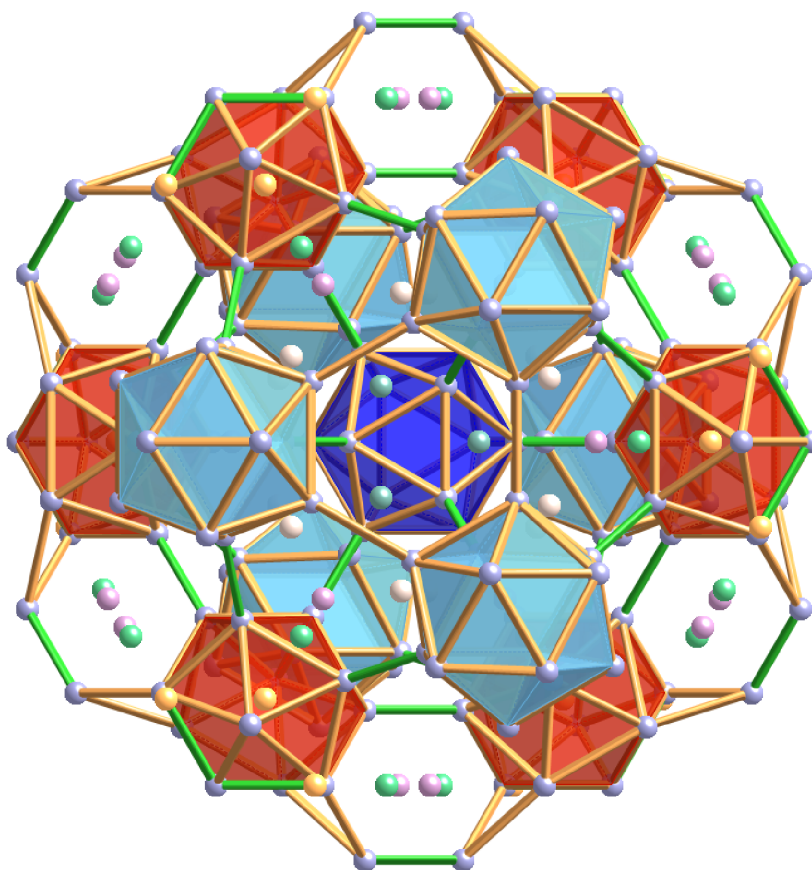


**Figure 2.** Structure of  $\beta$ -B (Pearson hR141) viewed from the body center (B15 site) to cell vertex along the (111) direction. Non-bonded atoms are partially occupied sites B16-B20. Partially occupied sites are shown in color: B13 (74.5% average occupancy cyan); B16 (27.2% pink); B17 (8.5% yellow); B18 (6.6% indigo); B19 (6.8% blue); B20 (3.7% orange).

Name	Pearson	Atoms	$V$	$E - E_\alpha$	$\Delta R$	Comments
$\beta$ -R	hR105	105	7.72	25.87	0.023	full occupation
$\alpha$ -R	hR12	12	7.18	0.00	0.002	full occupation
$\beta'$	hR111	105	7.69	13.02	0.013	B13bcdefB16a
$\beta'$	hR111	106	7.64	0.15	0.012	B13bcdefB16bd
$\beta'$	hR141	107	7.57	-0.86	0.005	B13bcefB16bdB17aB18a
$\beta'$	aP282	214	7.57	-1.75	NA	optimized supercell

**Table 1.** Structural data [10] including atoms per primitive cell, volume ( $\text{\AA}^3/\text{atom}$ ) and energy relative to  $\alpha$ -R (meV/atom).  $\Delta R$  ( $\text{\AA}$ ) measures the deviation of the symmetry-averaged relaxed positions from the crystallographically reported positions, averaged over the fully occupied Wyckoff positions. Comments list occupied sites using notation discussed in text. Structures labeled  $\beta'$  exploit partially occupied sites of hR111 or hR141 and break rhombohedral symmetry.

energy. To rigorously model the free energy of a phase we should evaluate both the full partition function which integrates the Boltzmann factor  $\exp -E/k_B T$  over all positions of all atoms. We will approximate this by integrating over small displacements (phonons) around nearly optimal discrete configurations  $C$ , as

$$e^{-F_{tot}/k_B T} = \int \prod_{i=1}^N d\mathbf{r}_i e^{-E/k_B T} \approx \sum_C e^{-(E(C)+F_{vib}(C,T))/k_B T} \quad (1)$$

where  $E_0(C)$  is the cohesive energy of configuration  $C$  and the vibrational free energy  $F_{vib}(C, T)$  depends on the phonon spectrum for each configuration  $C$ . The vibrational contributions will be approximated as being *independent* of configuration, yielding

$$F_{tot} \approx F_{vib}(C_{opt}, T) - k_B T \log Z_{conf} \quad (2)$$

where

$$Z_{conf} = \sum_C e^{-E(C)/k_B T}. \quad (3)$$

### Configurational free energy

The crucial step in determining the low temperature state of elemental boron is identifying the lowest energy configuration. Using electronic density functional theory we can accurately evaluate the energy of any specific configuration. Our precise methods, based on the VASP code [11] are described in Ref. [10]. As can be seen in in Table 1), the energy of  $\alpha$  lies below the energy of the original (hR105)  $\beta$  structure. To explain the observation of  $\beta$  as the stable structure, we must evaluate the energies of specific configurations of the more highly refined hR141 structure. Choosing the proper configuration to evaluate is a challenge. Within a single unit cell of hR141 there are 42 partially occupied sites, among which we must distribute 8 atoms, yielding more than  $10^8$  configurations that must be tested, in principle. Since each calculation takes approximately one day, we clearly need a way to simplify the search.

Our strategy is to first optimize a (hR111) structure [8] that contains only 16 Wyckoff positions, only two of which (B13 and B16) are partially occupied. Based on the reported 74.5% site occupancy of B13, and the 27.2% occupancy of B16, we consider structures with one or two vacant B13 sites (out of 6 per primitive cell) and one or two occupied B16 sites. From this we learn that it is favorable to place a single atom in each equilateral triangle of B16 atoms (i.e. one among B16abc and one among B16def, see Fig. 3). We also learn that when two B13 are vacant, the vacant sites prefer to be adjacent to each other.

Now consider the remaining sites, B17-20. Based on the reported 8.5% occupancy of B17 we attempt to occupy just a single site (out of six per primitive cell). The bond length of B17 from the nearest B13 site is only 1.57 Å, slightly too short for simultaneous occupancy. Hence we conjecture, and verify by total energy calculation, that the occupied B17 sites should be close to a vacant B13 site. Since the 6.8% reported occupancy of B18 is similar to B17, and the B17B18 bond is a favorable 1.62 Å length, we conjecture, and verify, the presence of a B17B18 bonded pair.

There are six available B17B18 pairs per primitive cell. One of the B13 sites collinear with this pair must be vacant, and one of the two nearby B13 sites must also be. Together with the three possible sites for each B16 atom, this yields  $6 \times 2 \times 3^2 = 108$  configurations to test. One of these (see Fig. 3) turns out to be the best structure we found. In particular, despite intensive efforts we found no lower energy structure utilizing either a B19 or a B20 site. The energy of our optimal structure turns out to be 0.86 meV per atom (0.092 eV per primitive cell) *below*  $E_\alpha$ . Among the 108 structures that obey the rules just stated, the energy differences were generally within about 0.1 eV per primitive cell. At a temperature  $T = T_m/2$ , where  $T_m$  is the melting temperature, fluctuations between these configurations should be active, yielding an entropy of  $k_B \log 108$  and reducing the free energy of  $\beta$  by a further  $k_B T \log 108 = 0.48$  eV per primitive cell.

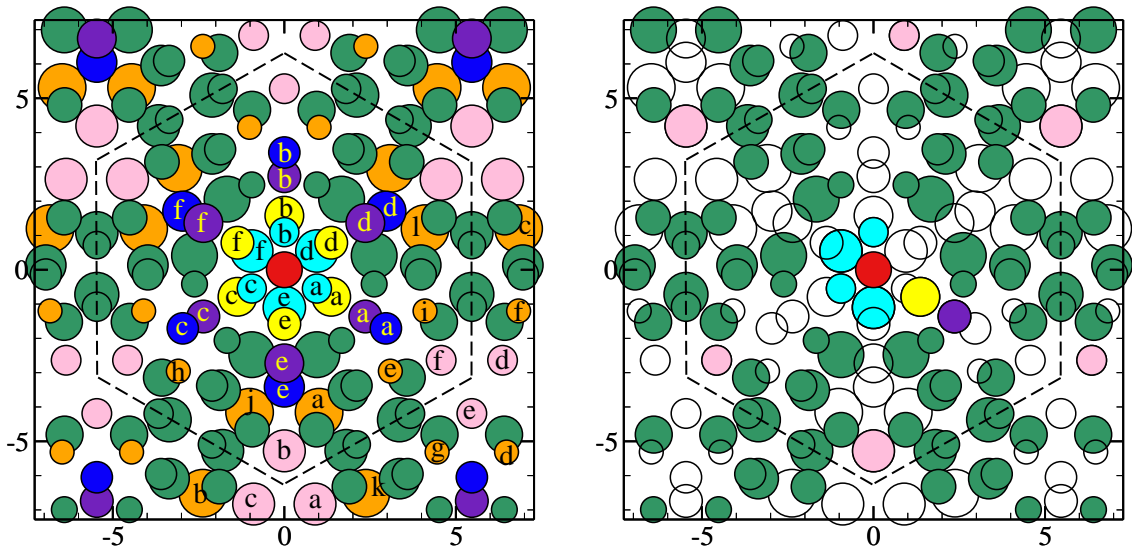


**Figure 3.** View of body center along (111) axis. Coloring as in Fig. 2: B13 (cyan); B16 (pink); B17 (yellow); B18 (indigo); B19 (blue); B20 (orange). (left) site labeling scheme; (right) optimal structure places atoms on sites “B13bdefB16bdB17aB18a”.

The electronic density of states offers potential insight into relative stability and optimal numbers of atoms. Fig. 4 illustrates the DOS of hR12 and hR105. Evidently  $\alpha$  is semiconducting (the Fermi energy lies at a gap) while  $\beta$  is predicted to be metallic (the Fermi energy lies in a band) in contradiction to experiment which finds  $\beta$  to be insulating. Placement of the Fermi energy in a gap can provide a means of lowering the total energy, potentially explaining  $E_\alpha < E_\beta$  while simultaneously indicating the possibility of modifying  $\beta$  to reduce its energy. An additional 5 electrons per primitive cell would place  $E_F^\beta$  in its band gap, indicating an additional 1.67 boron atoms are needed. However, the additional atoms in turn create new states, so in our hR141 structure  $E_F^{\beta'}$  remains below the gap by 1 electron per primitive cell.

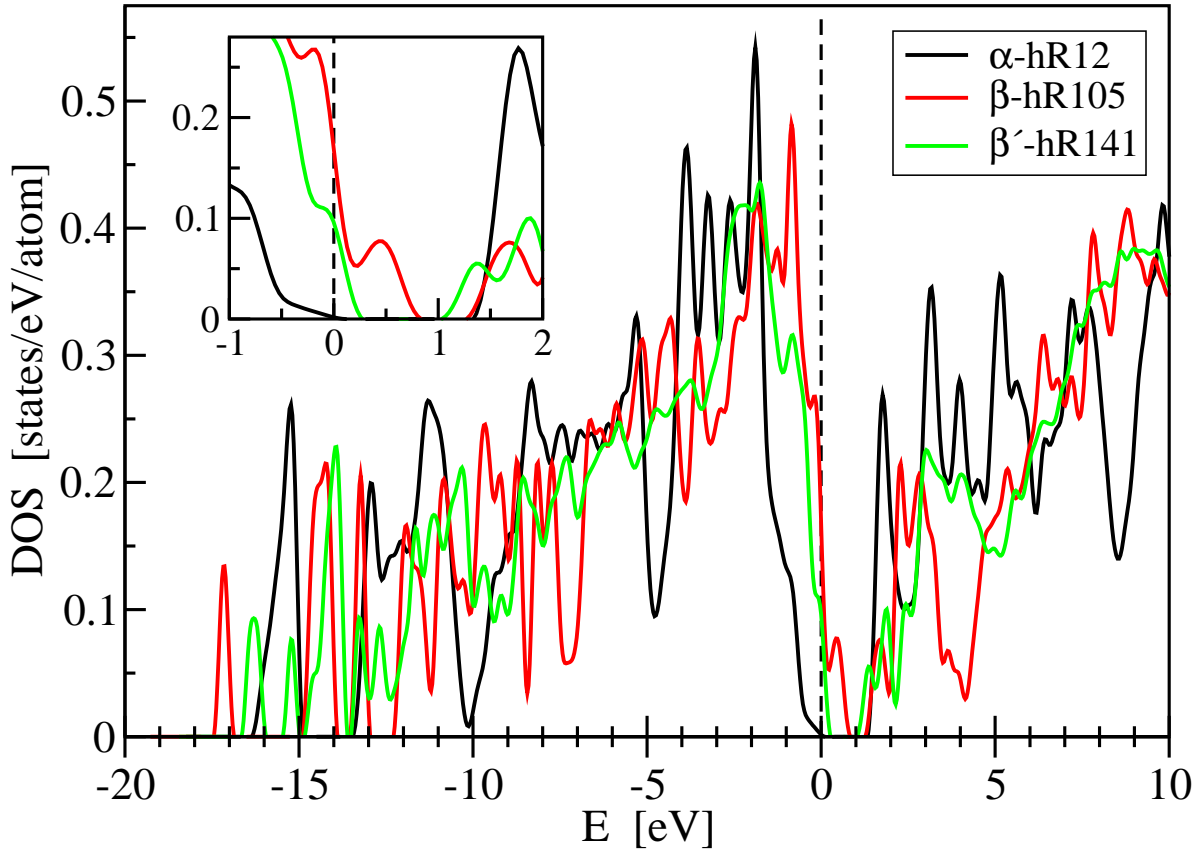


**Figure 4.** Single electron density of states for  $\alpha$  (hR12) and  $\beta$  (hR105). The Fermi energies ( $E_F^\alpha=6.15\text{eV}$ ,  $E_F^\beta=4.47\text{eV}$ ,  $E_F^{\beta'}=4.86\text{eV}$ ) have been shifted to zero to aid comparison. Note the DFT single electron band gap is not expected to match the experimentally observed electronic excitation band gap. Inset: enlargement of gap region.

While we believe we have found the optimal arrangements of atoms within a single primitive cell of  $\beta$ , we now test for a possible further reduction in energy by superlattice ordering. To do so, we combine two independent cells into a  $2 \times 1 \times 1$  supercell, and consider differing assignments of partially occupied sites in the two independent cells. To simplify our study, we only consider structures built out of our fundamental motif. Thus in each cell we replace a B13 pair with a B17/18 pair, but we vary the choices of specific pairs in the two cells. Since there are  $6 \times 2 = 12$  ways to move these pairs in a single cell, there are  $12^2 = 144$  ways to do it in our supercell, of which 22 are symmetry unrelated. For each of these 22 we obtain the optimal positions of the B16 atoms, resulting in 22 energies  $E_k$ , each of which has a multiplicity  $\Omega_k$  due to symmetry.

Several of our supercells achieve energy lower than our optimal primitive cell, with the best one (see Fig. 5) reaching energy 1.75 meV/atom below  $E_\alpha$ . Since superlattice ordering is favorable, we conclude that the optimal boron structure is not  $\beta$ , but some other structure  $\beta'$  that breaks the translational symmetry of  $\beta$ , leading to a larger lattice constant. Our particular supercell structure also breaks rhombohedral rotational symmetry (it has Pearson type aP214). Conceivably some other structure with superlattice ordering along the other two directions could restore rhombohedral symmetry, but still the translational symmetry of  $\beta$  would be broken.

According to the Landau theory of phase transitions, structures of differing symmetry must be separated by a thermodynamic phase transition. In the present case that means that a phase

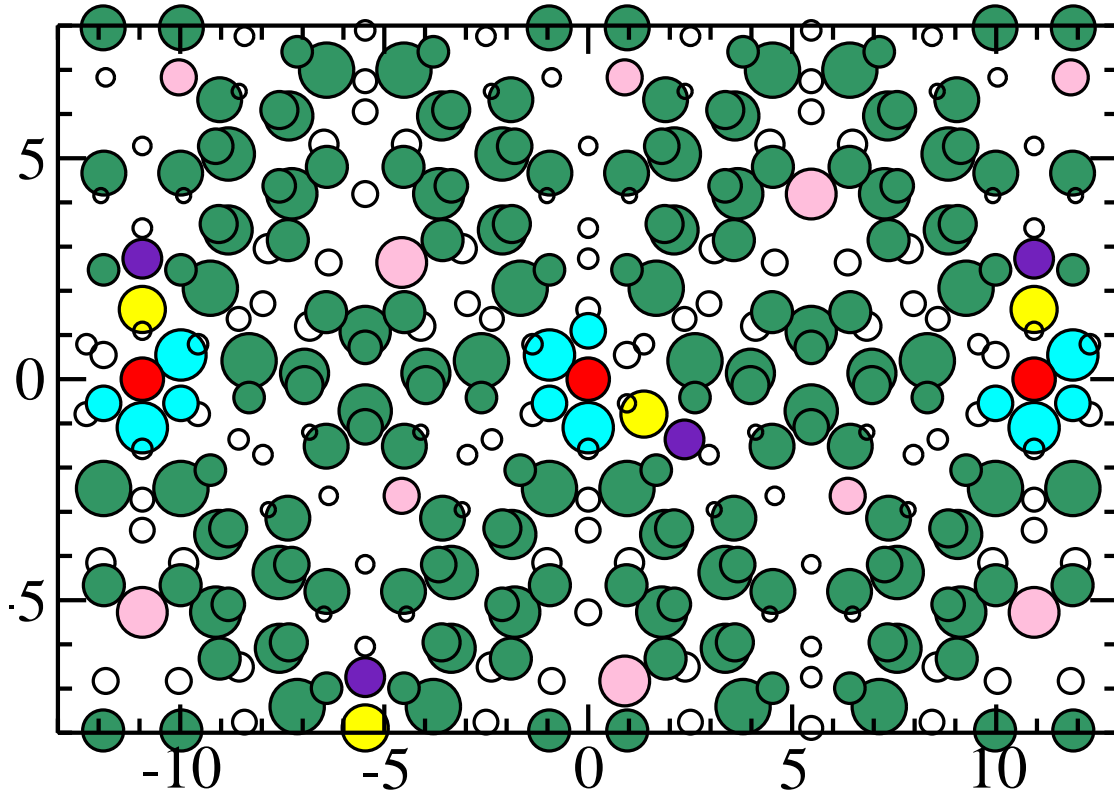


**Figure 5.** Optimal supercell as proposed in [10].

transition must separate the familiar  $\beta$  from the true low temperature phase,  $\beta'$ . To test this hypothesis, we evaluate the partition function

$$Z_{conf} = \sum_{k=1}^{22} \Omega_k e^{-E_k/k_B T} \quad (4)$$

using the energies and multiplicities obtained for the complete set of supercell models. Conventionally the canonical ensemble takes  $(N, V, T)$  as independent variables. Here consider only the dependence on  $T$ .  $N$  is fixed at the optimal value (214) for two primitive cells. The volume  $V$  is determined by relaxation of each specific configuration  $k$ , and is nearly a constant. Alternatively, this calculation can be considered in the isothermal-isobaric  $(N, P, T)$  ensemble with  $P = 0$ . Since the energies  $E_k$  are relaxed values, they hold only at  $T = 0\text{K}$ , and thus we neglect coupling of vibrations to the configurational free energy and we also neglect thermal expansion.

By thermodynamic differentiation we obtain internal energy, entropy and heat capacity, as illustrated in Fig. 6. Notice the entropic reduction in free energy reaches  $k_B T \log 12^2/214 = 4$  meV/atom, indicating complete freedom to sample all  $12^2$  differing configurations within the two cells by the time the temperature reaches  $T=2000\text{K}$ . evidently, around room temperature a phase transition occurs as fluctuations of atoms among different partially occupied sites stabilize the highly symmetric  $\beta$  phase over the energetically preferred but lower symmetry  $\beta'$  phase.

We only include a small subset of all low energy configurations in our sum (Eq. 4) because we select only the optimal B16 arrangement for each of our 22 supercell models. Hence the actual configurational entropy will be greater than the 4 meV/atom quoted above. Likewise, inclusion of a larger structural ensemble might shift the transition temperature somewhat. The

transition is broadened due to finite size effects, which can also shift the position of the heat capacity peak. So our entropy and transition temperatures are just crude estimates.

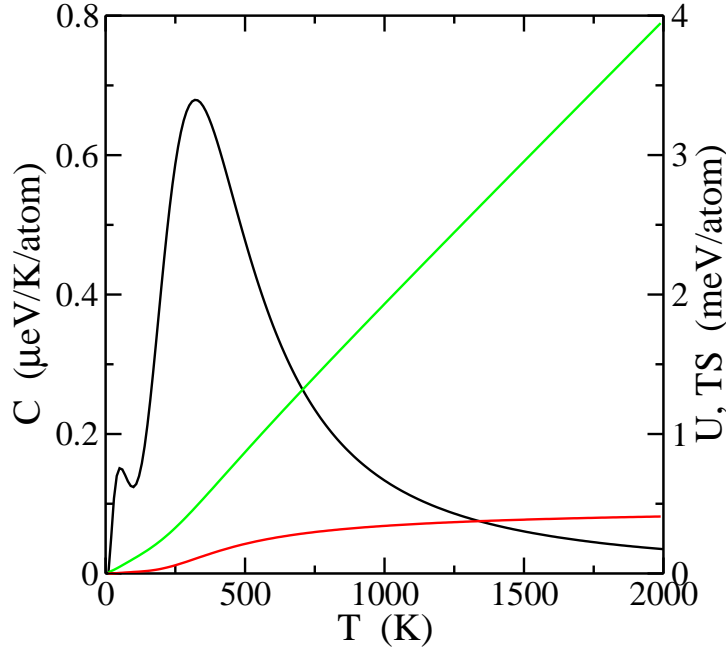


**Figure 6.** Thermodynamic data for supercell model [10]. Black line shows heat capacity, red line shows internal energy and green line shows  $TS$ , with  $S$  the entropy.

### Vibrational free energy

Vibrational free energy enhances the stability of both  $\beta$  and  $\beta'$  relative to  $\alpha$ . Owing to the complexity of the  $\beta$  structure, one previous calculation of vibrational free energy used only a single phonon  $k$ -point (the  $\Gamma$  point) to estimate the density of states [5]. Another [6] carried out both  $\Gamma$ -point and full Brillouin zone calculations, but only published the spectrum at the  $\Gamma$ -point. Phonon dispersion curves for  $\alpha$  have been previously calculated [12, 3], but again the full density of states was not published. Here we carry out true phonon calculations integrating over the full Brillouin zone.

Given vibrational density of states  $g(\omega)$ , the vibrational free energy is obtained by integrating the single mode free energy, resulting in

$$f_{vib}(T) = k_B T \int g(\omega) \log 2 \sinh \hbar\omega/2k_B T d\omega \quad (5)$$

Low frequencies, with  $\hbar\omega \ll k_B T$ , make negative contributions to the vibrational free energy. Structures with larger  $g(\omega)$  at low frequencies generally have lower vibrational free energy, lending greater thermodynamic stability. At sufficiently low temperature,  $f_{vib}$  approaches the quantum zero point energy

$$E_0 = \int g(\omega) \frac{\hbar\omega}{2k_B T} \quad (6)$$

Again, lower frequency modes lead to lower zero point energy and greater stability.

To calculate  $g(\omega)$  we evaluate the interatomic force constant matrix consisting of the second derivatives of total energy  $E$

$$\frac{\partial^2 E}{\partial \mathbf{R}_i \partial \mathbf{R}_j} \quad (7)$$



for atom positions  $\mathbf{R}_{i,j}$  within an interaction range that we took as 5.1 Å. Specifically, we extract these values from linear response, by displacing atoms from their equilibrium positions and calculating the resulting forces using VASP. Data is collected using our in-house phonon code. This matrix is then Fourier transformed at wavevector  $\mathbf{k}$  and then diagonalized yielding the dispersion relation  $\omega(\mathbf{k})$ . We evaluate  $\omega$  on a dense mesh in  $k$ -space, smear the values with gaussians of width 0.3 meV, then superpose the results.

All calculations are done within the harmonic approximation, holding the lattice parameters fixed at their optimal values. Some results including thermal expansion obtained within the quasiharmonic approximation are presented by Shang, *et. al.* [3].

The resulting  $g(\omega)$  for  $\alpha$  and for our optimized 107-atom  $\beta'$  structure are shown in Fig. 7. The DOS are similar over the low frequency (note energy  $E = \hbar\omega$ ) “acoustic” portion of the spectrum. Although  $\alpha$  exhibits some sharper features than  $\beta'$ , the contribution of these modes to thermodynamic stability is similar. The crucial difference in the spectra lies around 60 meV, where  $\alpha$  exhibits a gap between acoustic and optical modes, while  $\beta'$  possesses a high density of localized modes. This excess of low frequency modes leads to a reduction of  $f_{vib}$  for  $\beta'$  compared to  $\alpha$  that ranges from 3 meV/atom at low temperature (i.e. due to quantum zero point motion) to 15 meV/atom at  $T = 2000\text{K}$ .

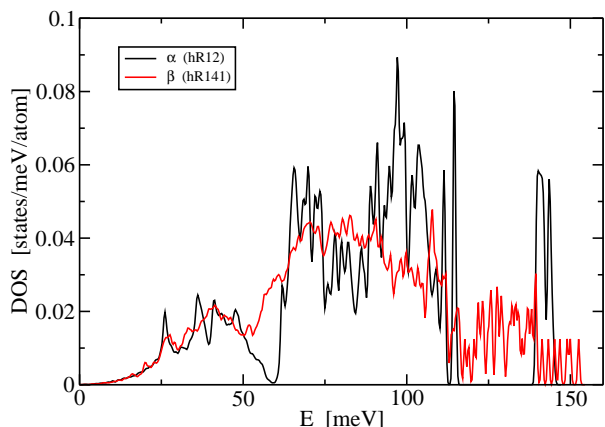


**Figure 7.** Vibrational densities of states for  $\alpha$  (black) and  $\beta'$  (red). Horizontal axis is phonon energy  $E = \hbar\omega$ . Vertical axis is density of states.

Localization of the modes is judged by their participation ratio,

$$PR = \frac{(\sum_k |u_k|^2)^2}{N \sum_k |u_k|^4} \quad (8)$$

where  $PR \sim 1$  indicates extended modes in which all atoms participate equally, and low PR indicates a localized mode in which only a few atoms are active.

For localized modes, the atom-projected density of states reveals which specific atoms are mobile at a given frequency. We find that the localized modes of  $\beta'$  in the energy range 55-65 meV lie predominantly on the B13 and B16 sites. The localized modes around 25 meV are predominantly associated with the B17 and B18 sites. Since these modes occur at low energies, these atoms are expected to be mobile at relatively low energies ( $\hbar\omega=60$  meV corresponds to  $k_B T$  at  $T=700\text{K}$ ). Indeed, in solid state molecular dynamics simulations [10] at  $T = 2000\text{K}$  precisely these atoms exhibited high mobility while the remaining atoms remained near their ideal positions.



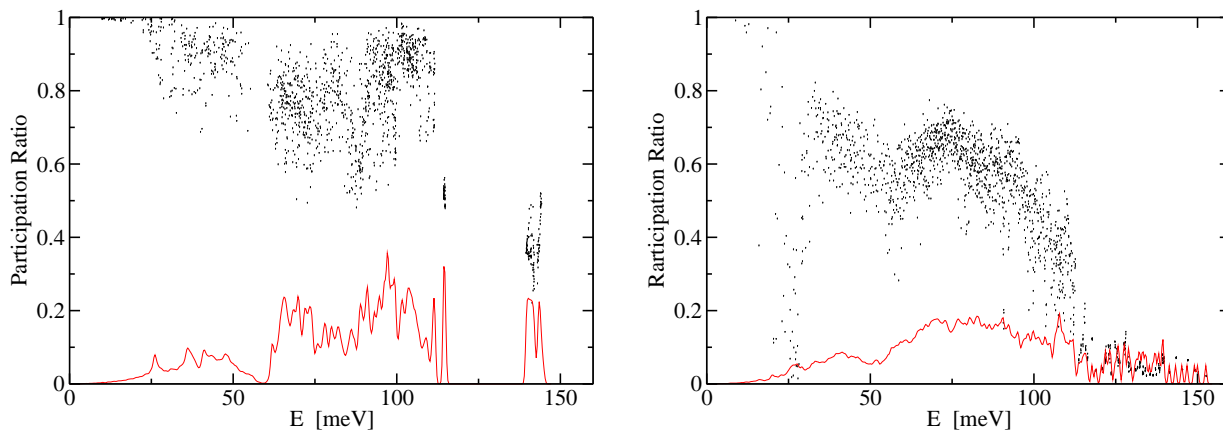


**Figure 8.** Participation ratios (see Eq. 8) of  $\alpha$  (left) and  $\beta'$  (right).  $PR$  is shown only for every 50th mode, and the densities of states are multiplied by 4, for visual clarity.

## Conclusions

In summary, we find that a specific arrangement of atoms among the partially occupied sites of  $\beta$ -rhombohedral boron achieve a lower total energy than  $\alpha$ . The optimal configuration within the primitive cell of  $\beta$  breaks rhombohedral symmetry, and further reduction in energy is possible by means of superlattice ordering. Thus we conclude that the true low temperature phase is not  $\beta$ -rhombohedral boron, but a related structure that we name  $\beta'$ . Careful experimental study of the X-ray diffraction pattern would be appropriate, seeking Bragg peaks or diffuse scattering (indicating partial ordering) in the vicinity of reciprocal space points where diffraction is forbidden by the symmetry of  $\beta$ . Selected area electron diffraction could also be helpful because the domain size of the ordered superlattice might be small, owing to the low temperature of the predicted ordering transition.

As temperature grows,  $\beta'$  transforms into  $\beta$  through a phase transition in the vicinity of  $T = 300\text{K}$ . A variety of circumstantial evidence supports the existence of a structural transition in  $\beta$  around this temperature. These are summarized in Ref. [13, 14] and include changes in photoabsorption spectra [15], internal friction [16] and dielectric properties [17, 18].

Within the  $\beta$  phase, the disorder of partial occupancy causes the internal energy to grow and to exceed the energy of  $\alpha$  by approximately 3 meV/atom by the time the temperature reaches  $T = 2000\text{K}$ . However, the entropy of  $\beta$  is sufficiently large that  $\beta$  has lower free energy than  $\alpha$  at all temperatures, up to melting. At  $T = 2000\text{K}$  the components of stability are the partial occupancy entropy of at least 4 meV/atom, and vibrational free energy of 15 meV/atom.

## Acknowledgments

We wish to acknowledge useful discussions with K. Shirai, N. Vast and H. Werheit. MM acknowledges support from grants VEGA-2/0157/08 and APVV-0413-06.

## References

- [1] Hoard J L and Hughes R E 1967 *The chemistry of boron and its compounds* ed Muetterties E L (Wiley) chap 2, p 25
- [2] Shirai K, Masago A and Katayama-Yoshida H 2006 *Phys. Stat. Sol. B* **244** 303–8
- [3] Shang S, Arroyave R and Liu Z K 2007 *Phys. Rev. B* **75** 092101
- [4] Mihalkovic M and Widom M 2004 *Phys. Rev. B* **70** 144107
- [5] Masago A, Shirai K and Katayama-Yoshida H 2006 *Phys. Rev. B* **73** 104102
- [6] van Setten M J, Uijtewaal M A, de Wijs G A and de Groot R A 2007 *J. Am. Chem. Soc.* **129** 2458–65

- [7] Hughes R E, Kennard C H L, Sullenger D B, and D E Sands H A W and Hoard J L 1963 *J. Am. Chem. Soc.* **85** 361
- [8] Callmer B 1977 *Acta Cryst. B* **33** 1951–4
- [9] Slack G A, Hejna C I and Kasper J S 1988 *J. Solid State Chem.* **76** 52–63
- [10] Widom M and Mihalkovič M 2008 *Phys. Rev. B* **77** 064113
- [11] Kresse G and furthmuller J 1996 *Phys. Rev. B*
- [12] Beckel C L, Yousaf M, Fuka M, Raja S Y and Lu N 1991 *Phys. Rev. B* **44** 2535–53
- [13] Wehrheit H and Franz R 1984 *Phys. Stat. Sol. B* **125** 779–84
- [14] Werheit H and Schmechel R 1998 *Landolt-Bornstein, Numerical data and functional relationships in science and technology Group III* vol 41C (Springer, Berlin) pp 3–148
- [15] Werheit H 1970 *Phys. Stat. Sol.* **39** 109
- [16] Tsagareishvili G V, Tavadze F N, Darsavelidze G S and Metreveli V S 1970 *Electron Tech.* **3** 281–90
- [17] Tsagareishvili O, Gabunia D and Chkhartishvili L 2008 *These Proceedings*
- [18] Tsagareishvili O A, Chkhartishvili L S and Gabunia D L 2009 *Semiconductors* **43** 18–25